Carboxylic and Dicarboxylic Acids Extracted from Crushed Magnesium Oxide Single Crystals

Friedemann Freund[*][§], Alka D. Gupta[§], and Devendra Kumar[§]

*   SETI Institute, NASA Ames Research Center, Moffett Field, CA 94035-1000, and
Department of Physics, San Jose State University, San Jose, CA 95192, USA

§   SETI Institute, 2035 Landings Drive, Mountain View, CA 94043, USA

Abstract. Carboxylic and dicarboxylic acids (glycolic, oxalic, malonic and succinic) have been extracted with tetrahydrofuran (THF) and H_2O from large synthetic MgO crystals, crushed to a medium fine powder. The extracts were characterized by infrared spectroscopy and ^1H–NMR. The THF extracts were derivatized with *tert*-butyldimethylsilyl (*t*-BDMS) for GC-MS analysis. A single crystal separated from the extract was used for an x-ray structure analysis, giving the monoclinic unit cell, space group $P2_1/c$ with $a_o = 5.543$ Å, $b_o = 8.845$ Å, $c_o = 5.086$ Å, and $\beta = 91.9°$, consistent with ß–succinic acid, $HOOC(CH_2)COOH$. The amount of extracted acids is estimated to be of the order of 0.1 to 0.5 mg/g MgO. The MgO crystals from which these organic acids were extracted grew from the 2860°C hot melt, saturated with CO/CO_2 and H_2O, thereby incorporating small amounts of the gaseous components to form a solid solution (ss) with MgO. Upon cooling, the ss becomes supersaturated, causing solute carbon and other solute species to segregate not only to the surface but also internally, to dislocations and subgrain boundaries. The organic acids extracted from the MgO crystals after crushing appear to derive from these segregated solutes that formed C–C, C–H and C–O bonds along dislocations and other defects in the MgO structure, leading to entities that can generically be described as $(H_x C_y O_z)^{n-}$. The processes underlying the formation of these precursors are fundamental in nature and expected to be operational in any minerals, preferentially those with dense structures, that crystallized in H_2O–CO_2–laden environments. This opens the possibility that common magmatic and metamorphic rocks when weathering at the surface of a tectonically active planet like Earth may be an important source of abiogenically formed complex organic compounds.

1. Introduction

Carbon is the champion of an enormously complex chemistry with itself and other low-z elements, in particular H, O and N. Electropositive with respect to oxygen, it forms CO and CO_2 and carboxy anions like carbonate, CO_3^{2-}. Other carboxy anions may exist in solid solution in non-carbonate minerals. Of particular interest are structurally dense phases such as olivine which grow in the upper mantle in an environment that is most certainly laden with CO/CO_2, H_2O, and other fluid phase components (Green, 1972; Thompson, 1992)

While H_2O undoubtedly enters into solid solution with nominally anhydrous minerals, forming hydroxyl anions, OH^-, or silanol groups, Si–OH (Aines and Rossman, 1984; Bell and Rossman, 1992; Wilkins and Sabine, 1973), CO and CO_2 have been considered incapable of entering structurally dense minerals as trace components (Mathez et al., 1987; Mathez and Delaney, 1981; Tingle et al., 1991; Tsong et al., 1985). This view stands in contrast to the thermodynamic laws governing phase equilibria: If a mineral grows in an environment laden with gases X, Y and Z, these gases will always become incorporated into the crystal structure, subject to specific partitioning functions (Helgeson et al., 1978; Iiyama and Volfinger, 1976). The solute concentrations may be small as in the case of noble gases which do not chemically interact with the solid matrix, but they will never be zero. In the case of CO and CO_2, considering how readily carbon bonds with oxygen, carbon is expected to be present in minerals that crystallized in CO/CO_2–laden environments. Since CO_2 is ubiquitous in natural systems as well as in laboratory and technical environments carbon may be a very common trace "impurity".

Studying the crystallization of forsterite from co–precipitated gels prepared by hydrolysis of metallo-organics, Park et al. (1994) observed an intermediate phase, structurally different from forsterite, which appeared to be stabilized by about 1 wt.% C. Chou et al. (1990) found carbon in ceramic substrates sintered from carbonate precursor materials. Shaw et al. (1990), Batson et al. (1991), and others (Kinoshita and Yamada, 1992) reported on carbon retention in perovskite-type YBaCu-oxides at a level of about one C atom per unit cell and a strong effect on the electrical conductivity of these superconducting materials. C atoms also enter non-oxide matrices such as silicon and GaAs, where they preferentially form dimers or bond to oxygen and/or hydrogen (Safonov et al., 1996; Shimura et al., 1985).

Magnesium oxide has served as a model for studying the incorporation of C in dense mineral structures. MgO crystals are routinely grown by the arc fusion method, where a melt pool is produced by the heat of a carbon arc burning in a cavity inside a compacted MgO powder bed (Butler et al., 1971). The MgO melt equilibrates with the atmosphere of the carbon plasma which is CO/CO_2–dominated but also contains H_2O, desorbing from

the MgO powder, and N_2 from the ambient atmosphere. When the MgO crystals begin to grow from such a melt, they must incorporate non-zero concentrations of all three low–z elements H, C and N.

Surface–analytical techniques, each with specific depth of information, have been used to study solute C in the MgO matrix. The $^{12}C(d,p)^{13}C$ nuclear reaction, which analyzes a 1-2 μm thick surface layer, showed substantial C concentrations in the bulk and segregation toward the surface during heating in ultrahigh vacuum (Wengeler et al., 1982). X-ray photoelectron spectroscopy (XPS) which is sensitive to the top 5-10 nm, confirmed the presence of solute C in experiments during which the XPS data were collected in ultrahigh vacuum over a wide temperature range, up to 900°C, beyond the range where adsorption of C-bearing molecules can be expected to occur (Kathrein et al., 1982). Using surface precoverage by ^{13}C–labelled CO_2, secondary ion mass spectrometry (SIMS), also conducted at high temperatures in ultrahigh vacuum, provided further evidence for solute C in the bulk and its segregation to the surface (Freund, 1986b). In spite of the wealth of information available, the idea that C does not occur as a trace impurity in dense structures like MgO and olivine has its proponents (Mathez et al., 1987; Tingle et al., 1991; Tsong et al., 1985). In this paper, we take a different, more chemical approach to solute C by analyzing organics that can be extracted from crushed arc fusion-grown MgO crystals by various organic solvents and by H_2O .

2. Method

The MgO crystals used in this study and designated DN-MgO were produced by DYNANIT-NOBEL AG, Troisdorf, Germany, in an industrial–scale arc fusion furnace where several tons of MgO of technical purity grade (98.0–98.5%) are molten, using 3-phase a.c. current and three 2 m long, 20 cm diameter graphite electrodes. After the electrodes are consumed and the arc has stopped, cm-sized MgO crystals grow rapidly from the very low viscosity, 2860°C hot MgO melt. Cooling to temperatures in the 300–600°C range takes several days. The MgO crystals are typically columnar, 6-10 mm diameter and up to 50 mm in length, arranged in bands alternating with layers of smaller, more isometric crystals, sometimes with small amounts of forsterite, Mg_2SiO_4, and monticellite, $MgCaSiO_4$, filling interstices between the MgO crystals. Major impurities in the MgO besides Si are Ca, Fe, Mn, Cr at levels of 100–1000 ppm.

Batches of 50 g hand-picked, columnar MgO single crystals were cleaned with $CHCl_3$ through reflux in a glass Soxhlet apparatus (prebaked at 450°C for 10 hrs), using cellulose thimbles precleaned with $CHCl_3$. The MgO crystals were then crushed manually in a clean porcelain mortar (prebaked at 450°C for 10 hrs) to a medium fine powder. The powder was placed back into the cellulose thimble and Soxhlet–extracted sequentially with three

solvents of increasing polarity for 16–24 hrs each: chloroform, acetone, and tetrahydrofuran (THF), using 250 ml of each solvent. Chloroform and acetone were HPLC–grade, purchased from Aldrich, and used as received. The HPLC–grade THF, also purchased from Aldrich, was refluxed and then distilled from sodium benzophenone. Full procedural blanks were performed using the same glassware, an empty thimble or a thimble filled with crushed, prebaked glass beads, and the same amounts of solvents.

H_2O extraction experiments were performed by placing 20 g crushed MgO powder in glass flasks (prebaked at 450°C for 10 hrs) in 150 ml H_2O, triple–distilled in a sub-boiling fused silica apparatus. The slurries were stirred at ambient temperature for 30 hrs with brief periods of sonication and two exchanges of 100 ml supernatant H_2O. The supernatants were centrifuged, combined and concentrated to about 2 ml by rotary evaporation. To remove cations, the concentrates were passed through a 3 x 95 mm ion exchange column (AG 50-X resing, 200-400 mesh, H^+ form, from Bio-Rad Laboratories), prewashed with HCl, NaOH solution and H_2O. The column was eluted with 150 ml H_2O, 100 ml 3.5 M NH_4OH solution and again 150 ml H_2O. The elute was concentrated by rotary evaporation and dried in a desiccator over NaOH. Full procedural blanks were performed with the same ion exchange column and same amounts of H_2O, HCl, NaOH and NH_4OH solutions.

The solvent extracts were reduced to near-dryness and characterized by infrared (IR) spectroscopy. IR spectra were obtained by drying a drop of the concentrates on a KBr single crystal, using a NICOLET 7199 FT-IR spectrometer. The extracts were further reduced to dryness. A portion was redissolved in deuterated solvents for proton nuclear magnetic resonance (^{1}H-NMR) analysis recorded on a Bruker WM-250 spectrometer at an operating frequency of 250.1 MHz with tetramethylsilane as an internal standard. Another portion of the extracts was used for gas chromatography-mass spectroscopic analysis (GC-MS) (Mawhinney, 1983; Silverstien et al., 1974).

The *tert*-butyldimethylsilyl (*t*-BDMS) derivatives for GC-MS analysis were prepared by adding 100 µl HPLC-grade acetonitrile and 100 µl *N*-Methyl-*N*-(*tert*-butyl-dimethylsilyl)trifluoroacetamide, containing 1% *tert*-butyldimethyl chloride (MTBSTFA reagent, Regis Chemical), to the dry extracts, sealing them immediately in screw-top Teflon-lined tubes, followed by heating to 80°C for 30 min and cooling to room temperature before injection. The analyses were carried out on a HEWLETT-PACKARD 5890A GC fitted with a 30 m x 0.25 mm fused silica capillary column coated with OV-17 (J&W Scientific). The operating conditions were initial 70°C and 10°C/min to 230°C. The mass spectra were obtained with an HP 5971 mass selective detector, operating at 70 eV with 280°C interface temperature.

3. Results

The IR spectra of the sequentially obtained chloroform, acetone and THF extracts of crushed DN–MgO single crystal powder are shown in **Figure 1a**. The IR spectra provide evidence for organics through absorption bands in the 2850-3000 cm^{-1} region, indicative of C-H stretching modes. Spectrum (3) of the THF extract gives a number of partly overlapping, unresolved bands in the 600–1500 cm^{-1} fingerprint region, an intense band at 1723 cm^{-1}, indicative of a carbonyl group of saturated aliphatic carboxylic acid dimers (Sadtler, 1987; Silverstien et al., 1974), and a strong double band in the C-H stretching region at 2890 and 2960 cm^{-1} merging with a strong, broad O–H stretching band between 3000–3600 cm^{-1}, indicative of H-bonded carboxylic acid groups, –COOH. Spectrum (2) of the acetone extract gives two sharp, though relatively weak bands in the C–H stretching region at 2850 and 2920 cm^{-1} plus minor bands at 2870 and 2955 cm^{-1}, plus a strong band at 1354 cm^{-1}. Spectrum (1) of the spectrum of the chloroform abstract has intense bands in the C–H stretching region at the same wavenumbers, and a number of bands in the 600–1500 cm^{-1} region. By contrast, the solvent residues and blank extracts produced negligible amounts of residual organics. In **Figure 1b** we show in (1) the results of a full procedural blank with THF as the solvent, performed with about the same amount of crushed Pyrex glass powder. in (2) a very thick THF extract, and in (3) once more the IR spectrum of the THF extract from the crushed MgO crystals. Because THF is a reactive solvent it may be sensitive to oxidation during reflux boiling in the presence of atmospheric O_2. The near–absence of IR bands in the residue spectrum of the glass procedural blank indicates that THF did not react under the conditions used in our experiments.

Tetrahydrofuran Extracts

The THF extract was concentrated and purified by addition of chloroform with which it is partially immiscible. By separating the chloroform after shaking and allowing it to slowly evaporate, colorless crystals began to form. Some grew up to 1 mm in size as shown in **Figure 2**. Their melting point was 189–190°C, close to the 188°C reported for succinic acid (Weast and Astle, 1985). The mass spectrum, obtained with a FINNIGAN 4000 mass spectrometer with a direct insertion probe, yielded an ion at m/z 119 along with fragments at m/z 73 and 101. The m/z 119 peak is interpreted as the (M+1)$^+$ ion of succinic acid (Cornu and Massot, 1975), while those at m/z 73 and 101 indicate loss of a carboxylic group, –COOH, and a hydroxyl group, –OH, respectively. After redissolution in THF and evaporation of the solvent an IR spectrum of these crystals was obtained, shown in **Figure 3**, exhibiting a number of sharp bands, consistent with the reported bands for succinic acid (Schrader and Meier, 1974) summarized in the inset in **Figure 3**. The

^{1}H-NMR spectrum of a solution in deuterated tetrahydrofuran (THF-d_8) shows a singlet at 2.54 ppm with reference to tetramethyl-silane, corresponding to methylene groups, $-CH_2-$, and a D_2O–exchangeable broad singlet at 10.37 ppm, corresponding to carboxylic acid groups, $-COOH$, at an intensity ratio consistent with the ^{1}H–NMR spectrum of succinic acid. A hand-picked, untwinned single crystal, about 100 μm in size, was used for an x-ray structure analysis, performed on a CAD-4-circle ENRAF-NONIUS goniometer, with Cu Kα_1 radiation. The monoclinic space group was determined to be $P2_1/c$ with unit cell dimensions $a_0 = 5.543$ Å, $b_0 = 8.845$ Å, $c_0 = 5.086$ Å, with ß $= 91.9°$, close to the reported values for ß–succinic acid, $HOOC(CH_2)COOH$, reported by Broadley et al. (1959) $a_0 = 5.519$ Å, $b_0 = 8.880$ Å, $c_0 = 5.126$ Å, with ß $= 91.3°$.

The THF extract was derivatized, using t-BDMS, and analyzed by GC-MS. In the mass spectra of t-BDMS derivatives, the parent ions M^+ are usually of low intensity or absent. Instead, a strong $(M-57)^+$ peak and a weak $(M-15)^+$ peak are observed, due to the loss of a t-butyl group and hydroxyl group, respectively (Corey and Venkateswarlu, 1972). Peaks at m/z = 73, 75, 115, 147, and 187 are also characteristic for fragments of t-BDMS and trimethylsilyl derivatives (Butts and Rainey, 1971; Mawhinney, 1983). Of these, the 73, 147 and 189 m/z ions arise from fragments retaining two or more silyl groups, whereas the 75 m/z fragment is indicative of the monosilylated ion.

The GC trace shown in **Figure 4** exhibits several peaks, three of which at retention times 11.23, 12.39, and 14.03 min, respectively, have been identified on the basis of their mass spectra (Butts and Rainey, 1971; Mawhinney, 1983) and by comparison with authentic compounds as oxalic acid, $HOOCCOOH$, malonic acid, $HOOCCH_2COOH$, and succinic acid, $HOOC(CH_2)_2COOH$. A fourth GC peak, at 8.94 min, has been identified as glycolic acid, $HOCH_2COOH$. **Figure 5** shows the corresponding mass spectra. GC–MS analysis of the procedural blanks occasionally showed very small amounts of glycolic acid extracted from the empty thimble but none of the other acids listed. The traces of glycolic acid observed in some blanks are believed to come from the GC inlet system.

In view of the large amounts of organic acids extracted, of the order of 1-5 mg per 50 g MgO, and because the procedural blanks yielded no carboxylic and dicarboxylic acids (except for traces of glycolic acid extracted from the thimble), we can rule out adventitious contamination in the laboratory as a possible source.

The H_2O extract of MgO was reduced to dryness, t-BDMS–derivatized and analyzed in an identical manner as the THF extracts. Oxalic, malonic and succinic acids were identified on the basis of retention times and mass spectra and by comparison with authentic samples of oxalic and succinic acids. The total amount of acids extracted by H_2O was less than those extracted by THF. The reason appears to be that, because of the high basicity of the aqueous solution in equilibrium with the MgO slurry, pH ≈ 8.5, most

organic acids are strongly bound to the MgO–Mg(OH)$_2$ residue. GC–MS analysis of the procedural blank H$_2$O extract showed none of the organic acids listed.

Since the same organic acids are extracted from the MgO single crystal powder by THF and by H$_2$O, albeit in different quantities, we can rule out that these compounds might have formed as a result of a reaction between THF and the MgO surface. This leads us to propose that the organic acids are products of the MgO crystals grown from the CO/CO$_2$–saturated melt and cooled to room temperature.

While laboratory contamination is always a major concern when dealing with organics extracted from the surface of a powder, it is highly unlikely that carboxylic and dicarboxylic acids can become adsorbed on the MgO surface or could have formed as a result of reactive chemisorption involving volatile C-bearing compounds from the ambient atmosphere. To confirm it, we exposed 50 g freshly crushed MgO powder for a very long time, 18 months, to the laboratory atmosphere and subjected it then to the same extraction procedure as described above. The rationale for this experiment was that, if contamination occurred, it would most likely increase with time. The MgO powder was stored in an open glass beaker covered with an Al foil. While the Al foil protected against infall of particulate matter, in particular dust, it allowed for exchange with the laboratory atmosphere. After 18 months, the 50 g sample was extracted with THF. The extract was reduced in volume and a drop dried on a KBr crystal plate for IR analysis. The extracted MgO powder was then dried and crushed to a finer powder so as to create new fracture surfaces. The finer powder was re-extracted with THF, and its extract analyzed by IR.

In **Figure 6** the IR spectra are combined of the three THF extracts: (1) from the freshly crushed MgO powder recorded in Dec. 1996, (2) from the sample stored for 18 months, until May 1998, and (3) from the same 18 months old MgO sample recrushed to a finer powder and re-extracted.

Spectrum (1) exhibits the characteristic bands of carboxylic acids mentioned above. Spectrum (2) shows generally the same bands with some changes in relative intensities, suggesting a decrease of the amount of extractable organics over the 18 months exposure time. Noteworthy is the decreased intensity of the broad band between 3000–3600 cm^{-1}, indicative of –COOH, relative to the intensity of the C–H bands around 2850–2950 cm^{-1}. A new band appeared around 1610 cm^{-1} (marked by a vertical arrow). Spectrum (3) shows that, upon recrushing the extracted 18 months old powder and re-extracting it with THF in he same manner as before, the band intensity in the 3000–3600 cm^{-1} region increases markedly, while the band at 1610 cm^{-1} is no longer observable.

The decrease in the band intensity of the broad –COOH band between 3000–3600 cm^{-1} and the appearance of the 1610 cm^{-1} band suggests that the acid groups converted to

carboxylate, $-COO^-$, e.g. to Mg–salts, the antisymmetric C–O stretching frequency of which gives rise to a strong band around 1610 cm^{-1} (Schrader and Meier, 1974).

Though the intensities of IR bands recorded from the same number of drops of extracts can only be taken as a crude measure of quantities, the amount of extractable organics seems to have decreased over 18 months storage in laboratory air. The extract was derivatized for GC-MS analysis. The results show a drastic decrease in the concentration of extractable acids, consistent with the suggestion that the acids had converted to carboxylate salts which are no longer soluble in THF. After recrushing, the amounts of extractable acids increased again noticeably though not to the level of 18 months earlier.

These observations add to the argument that the carboxylic and dicarboxylic acids extracted by THF from the freshly crushed MgO crystals are not the result of adventitious gas phase contamination or of reactive chemisorpion from the laboratory atmosphere.

The IR spectrum of the acetone extract was relatively simple (**Figure 1**) with one strong band at 1354 cm^{-1} and C–H bands at 2850 and 2920 cm^{-1}. The ^{1}H-NMR spectrum indicates -CH$_3$ and -CH$_2$- groups in various environments. The absence of coupling in the ^{1}H–NMR spectrum means that these groups are either separated by a heteroatom or a C atom carrying no protons, suggestive of an oxygen-heterocyclic compound. A more detailed report on this compound will be published elsewhere.

The IR spectrum of the chloroform extract shows a multitude of bands (**Figure 1**), all of which suggest aliphatic hydrocarbons. The ^{1}H-NMR spectrum indicates the presence of aliphatic -CH$_3$ and -CH$_2$- groups. No signal was observed in the aromatic region. A more detailed report on this compound will be published elsewhere.

4. Discussion

The MgO crystals used to produce the crushed powder samples for our extraction experiments grew from a 2860°C hot MgO melt pool, self-contained in a compacted MgO powder bed. The melt pool was generated by a carbon arc plasma and therefore stood in equilibrium with its gases, foremost CO/CO$_2$ but also H$_2$O from moisture released from the MgO powder bed. At the high temperature of the melt no organic molecules can exist. Whenever a situation arises that a crystal grows from a melt that saturated with gases, in particular with reactive gases such as H$_2$O, CO/CO$_2$, some of these gases must become incorporated into the crystal structure.

The underlying principle is illustrated in **Figure 7** representing a section of an AO–BO phase diagram where AO is a high melting oxide and BO an oxide component which may be a liquid or a gas at ambient conditions such as H$_2$O and CO/CO$_2$ respectively. The addition of BO causes the melting point, T$_m$, of the pure compound AO to be depressed to T$_{cryst}$. Instead of pure AO, an AO–BO solid solution is formed (ss, light grey). Such a

solid solution can be formally described by a substitution of cations A^{n+} by B^{m+} in a relative proportion satisfying neutrality, normalized to a constant number of oxygens.

If AO is MgO and BO is CO, carbon would be treated as a divalent solute, and its incorporation into the MgO structure at a concentration level δ requires δ Mg^{2+} vacancies:

$$MgO + \delta\ CO = Mg_{1-\delta}C_\delta O + \delta\ MgO \qquad [1]$$
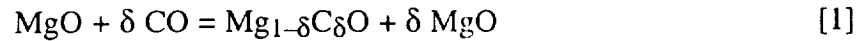
If BO is CO_2, carbon is treated as a tetravalent solute, requiring 2δ Mg^{2+} vacancies:

$$MgO + \delta\ CO_2 = Mg_{1-2\delta}C_\delta O + 2\delta\ MgO \qquad [2]$$
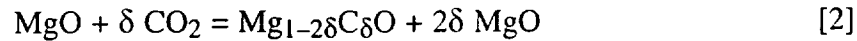
The equilibrium solute concentration δ is a function of temperature. Upon cooling, as long as equilibrium can be maintained, the ss composition changes along the equilibrium line by degassing BO and constantly adjusting the vacancy concentration in the AO bulk. Sooner or later during cooling, however, a point will be reached, designated as $T_{critical}$ in **Figure 7**, when the equilibrium can no longer be maintained because the necessary adjustments in the ss bulk do not keep up with the cooling rate. At this point, the solid solution freezes, causing the solid solution (ss) to leave thermodynamic equilibrium and to become a supersaturated solid solution (sss, dark grey). In the sss field, the system can marginally lower its total energy by continuing to segregate some excess solutes and excess cation vacancies. If the outer surface is too far away, segregation will proceed over shorter distances towards dislocations, subgrain boundaries and other defects in the AO bulk where strain can be accommodated. Since the process involves not only solute segregation but also vacancy segregation, it can generate its own internal surfaces by vacancy clustering, e.g. the formation of cavities.

The consequences of such a process can be seen in **Figure 8a**, showing a 20 mm large, high purity (99.9%) MgO crystal grown in a laboratory arc fusion furnace. The crystal is bounded on the right and the left by its growth surfaces. A portion of the sintered MgO from the melt pool wall is discernible in the upper left. Because of the high purity grade, less than 500 ppm cationic impurities, the solutes are mostly those which derive from the ss formation with the gases dissolved in the MgO melt, primarily CO/CO_2 and H_2O.

During cooling the ss crystal must have followed for some time the equilibrium line in **Figure 7**, allowing the solute gaseous components to degas from a 2–4 mm wide rim. When it reached $T_{critical}$, the ss crystal must have quickly become supersaturated, leading in its interior to pervasive cavity formation, presumably by vacancy clustering and solute precipitation. **Figure 8b** depicts the interior of this MgO crystal at a higher magnification (100 x) showing isolated cavities, about 5-10 μm in size, and a dense network of curved subgrain boundaries decorated by cavities the sizes of which reach the limit of optical resolution even at 1000 x.

While a detailed description of the "architecture" of the internal segregation network is beyond the scope of this paper, the visibility of cavities and cavity–decorated subgrain boundaries is relevant to the topic under discussion.

IR spectra of the cloudy interior of MgO crystals do not yield any evidence for gaseous CO_2 or H_2O which should be the primary degassing products filling the cavities. Even heating such cloudy MgO crystals to temperatures at which Mg–hydroxy-carbonates and $MgCO_3$ would decompose which might have formed on the cavity walls, does not produce CO_2 or H_2O gas (Freund and Wengeler, 1982).

Figure 9 shows the IR spectrum of an arc fusion–grown MgO crystal between 2750–4250 cm^{-1}, 8 mm thick and of high purity (99.9%), recorded at room temperature. The spectrum is dominated by O–H stretching bands. The bands at 3300 cm^{-1} and 3560 cm^{-1} are due to one OH^- and two OH^- at Mg^{2+} vacancy sites, respectively (Freund and Wengeler, 1982). The broad band (stippled) has been assigned to OH^- on a regular O^{2-} site. In addition there is diagnostically distinct H–H stretching band near 4150 cm^{-1}, due to a Qr1(0) combination band of molecular H_2 with a low frequency MgO lattice mode (Warren et al., 1980), and bands in the C–H stretching region between 2800–2950 cm^{-1}. The latter are associated with C–H–bearing entities in the MgO bulk. Upon heating to 400°C, they disappear but reappear at room temperature over a time period of several weeks to months (unpubl. results).

Combining this information with the general knowledge derived from thermodynamics of supersaturated solid solutions, we can return to the main subject of this report, the extraction of carboxylic and dicarboxylic acids from the crushed powder of arc fusion grown MgO crystals.

It appears certain that the dilute solid solution between MgO and CO/CO_2 that forms during crystal growth from a CO/CO_2–saturated melt does not lead to carbonate anions, CO_3^{2-}, as solute species. Being planar and carrying a total of 2– charges spread over three oxygens, the CO_3^{2-} does not fit well into the MgO structure where three oxygens represent a total of 6– charges. Instead, it has been proposed (Freund and Wengeler, 1982) that the solute species is CO_2^{2-}, a chemically reduced carboxyanion with C sitting off–center in an Mg^{2+} vacancy site. CO_2^{2-} is a carboxylate anion, formally $CO + O^{2-} = CO_2^{2-}$, isoelectronic with the •CF_2 radical, bent with an O-C-O angle of about 125° and a C–O distance of 1.27 Å. The IR band due to its antisymmetric C–O stretching vibration lies in the 1550–1610 cm^{-1} region (Schrader and Meier, 1974). The IR spectrum of CO_2^{2-} anions has been measured in inert gas matrices (Kafafi et al., 1984) but the C–O stretching band of a CO_2^{2-} imbedded in and strongly coupled to the MgO structure is epxected to be excessively broadened, inobservable in the presence of MgO combination and overtone bands in the same spectral region.

Indirect evidence for the CO_2^{2-} anion has been obtained from the studies mentioned earlier where the $^{12}C(d,p)^{13}C$ nuclear reaction was used to measure the C concentration in a 1–2 μm thick surface layer of MgO crystals during heating to temperatures up to 700°C and an IR study of the concurrent changes the O–H stretching band intensities arising from OH$^-$ in the MgO bulk (Freund, 1986a; Wengeler et al., 1982). Around 500°C the (d,p) data indicate a surge of C mobilized inside the MgO crystal and diffusing to the surface. At the same temperature the intensity of the IR band from single OH$^-$ at Mg^{2+} vacancies, increases multifold (Freund and Wengeler, 1982). Combining these two observations, it was suggested (Freund, 1987) that the off–center C atoms in the octahedrally coordinated Mg^{2+} vacancy sites, bonded to two O$^-$, transit into tetrahedrally coordinated interstitial sites, bonded to one O$^-$ and forming a complex withing the MgO structure which can be described as CO$^-$ carboxy anion. As the C atoms vacate the Mg^{2+} vacancy sites, OH$^-$ settle in, thereby causing the observed increase in O–H stretching band intensity (Freund and Wengeler, 1982).

CO$^-$ with C on tetrahedral sites account for the diffusive mobility of the C atoms which can be described as a co-diffusion of a C atom and a defect electron on the O^{2-} sublattice (Freund, 1986b). In this way the C atom moves through the stationary dense O^{2-} packing by bonding transiently to O$^-$. Chemically, the C in CO$^-$ is more reduced that in CO_2^{2-}.

Because the C atom is thus diffusively mobile, it can respond to the thermodynamic driving force that is a hallmark of the supersaturated solid solution. This driving force tends to decrease the concentration of "impurities" in the bulk, causing them to segregate to the crystal surface or, if the surface is too far away, to internal segregation sites such as dislocations, subgrain boundaries etc. This purely solid state process concentrates even very dilute "impurities" in the segregation sites such as the solute C which may achieve an average bulk concentration of 100 ppm. This relatively high concentration level of solute C in MgO is supported by a wet–chemical total carbon analysis in MgO which gave a value around 50 wt.–ppm, equivalent to about 150 at.–ppm (Freund 1986b). As more and more C atoms arrive at the segratation sites, they become locally concentrated. Eventually they will start tying C–C bonds to form in C–bearing precipitates decorating dislocations and subgrain boundaries. Because the segregation of C is also accompanied by segregation of H_2, C and H_2 come close and can begin reacting within the confinement of a dislocation core or a dislocation array of a subgrain boundary. Through these reactions, CO$^-$ would bond to other CO$^-$ and to H_2, leading to "organic" precipitates that can be generically described as $[H_xC_yO_z]^{-n}$.

These H–C–O precipitates, formed in the narrow confinement of dislocations and other defects, appear to be the entities from which the organic molecules derive on which we have reported here. Upon crushing the dislocations and subgrain boundaries decorated by

$[H_xC_yO_z]^{-n}$ become exposed, causing the precipitates become accessible to solvent and H_2O extraction. In view of the glycolic acid and dicarboxylic acids from oxalic to succinic extracted from the MgO powder, it is tempting to suggest that they arose by 2, 3 and 4 CO^- reacting with H_2 inside the MgO matrix and possibly with traces of H_2O during solvent extraction to give the C_2, C_3 and C_4 organic acids, $HOCH_2COOH$, $HOOC$-$COOH$, $HOOC(CH_2)COOH$, and $HOOC(CH_2)_2COOH$, respectively.

A lingering suspicion may remain that, despite our best efforts to control the sample preparation and solvent extraction at each step of the process, the dominance of succinic acid in the THF extracts may be caused by oxidation of THF in the presence of air, catalyzed by basic sites on the MgO surface. This concern cannot be relieved by operational controls alone because they lack the basic sites. We are planning to repeat the Soxlets extraction with deuterated THF and will report on the results in a short note.

The processes described in this paper are fundamental in nature and based on thermo-dynamic principles that govern (i) the formation of solid solutions between a high melting oxide AO and gas-fluid phase components BO (H_2O and CO_2) when AO crystallizes in H_2O/CO_2-laden environments, and (ii) the supersaturation of this solid solution during cooling with its ensuing driving force for segregation. What had not been previously recognized is the *in situ* redox conversion of the solutes deriving from the gas–fluid phase components H_2O and CO_2, leading to H_2 molecules and chemically reduced C inside the crystal matrix. The co-segregation and eventual reaction of H_2 and C to form $[H_xC_yO_z]^{-n}$ precipitates along dislocations are a direct consequence of solid state supersaturation.

MgO has thus served us as model for a more general phenomenon. Since the solid state processes described are fundamental, they surely take place in rock–forming minerals as well which crystallize in H_2O–CO_2–laden magmas or recrystallize in metamorphic, H_2O–CO_2–laden environments. This encompasses the vast majority of crustal rocks and all upper mantle rocks. We therefore must be open to the possibility that minerals in such common rocks contain the same or similar $[H_xC_yO_z]^{-n}$ precipitates as the laboratory-grown MgO crystals. When subjected to weathering at the Earth's surface, these minerals will discharge their complement of abiogenically formed complex organics.

Whether the concentrations of $[H_xC_yO_z]^{-n}$ precipitates in different mineral phases are of the same magnitude as in MgO is currently unknown. These values will critically depend upon a range of factors which include the amounts of H_2O and CO_2 components incoroporated during crystallization, the extent of the *in situ* redox conversion, and the degree of supersaturation. Many minerals in crustal rocks, such as feldspars, have much less dense structures than MgO. Though there is evidence that the redox conversion also takes place in these more open structures, once the redcued solute species are formed, they are less driven to segregate. This is because the denser the structure, the stronger the

driving force for segregation. Unfortunately, no experimental data on organics that may be extractable from feldspars and similar minerals are currently available.

The only natural mineral for which we have completed a similar study as described here is olivine, using 10–20 mm sized, gem–quality upper mantle derived olivine crystals as starting material. Olivine has in common with MgO a very dense structure. It was therefore not surprising to find that organics were extractable from crushed olivine crystals, though the compounds extracted show a different product distribution. The results, to be published elsewhere, confirm the general conclusions reached in this paper. They alert us to the possibility that, on a tectonically active planet like Earth, rocks subjected to weathering represent a potentially large source of abiogenically formed complex organic compounds.

5. Acknowledgments

References

Aines, R. D. and Rossman, G. R.: 1984, *J. Geophys. REs.* **89**, 4059.

Batson, P. E., Shaw, T. M., Dimos, D. and Duncombe, P. R.: 1991, *Phys. Rev. B.* **43**, 6236.

Bell, D. R. and Rossman, G. R.: 1992, *Science.* **255**, 1391.

Broadley, R. J., Cruickshank, D. W., Morrison, J. D., Robertson, J. M. and Shearer, H. M. M.: 1959, *Proc. Royal Soc. (London).* **A251**, 441.

Butler, C. T., Sturm, B. J. and Quincy, R. B.: 1971, *J. Cryst. Growth.* **8**, 197.

Butts, W. C. and Rainey, W. T.: 1971, *Anal. Chem.* **43**, 538.

Chou, N. J., Zabel, T. H., Kim, J. and Ritsko, J. J.: 1990, *Nucl. Instr. Meth. Phys. Res.* **B45**, 86.

Corey, E. J. and Venkateswarlu, A.: 1972, *J. Am. Chem. Soc.* **94**, 6190.

Cornu, A. and Massot, R.: 1975, *Compilation of Mass Spectral Data*, London, Heyden.

Freund, F.: 1986a, *J. Cryst. Growth.* **75**, 1001.

Freund, F.: 1986b, *Phys. Chem. Minerals.* **13**, 262.

Freund, F.: 1987, *Phys. Chem. Minerals.* **15**, 1.

Freund, F. and Wengeler, H.: 1982, *J. Phys. Chem. Solids.* **43**, 129.

Green, H. W.: 1972, *Nature.* **238**, 2.

Helgeson, H. C., Delany, J. M., Nesbitt, H. W. and Bird, D. K.: 1978, *Amer. J. Sci.* **278A**, 1.

Iiyama, J. T. and Volfinger, M.: 1976, *Mineral. Mag.* **40**, 555.

Kafafi, Z. L., Hauge, R. H., Billups, W. E. and Margrave, J. L.: 1984, *Inorgan. Chem.* **23**, 177.

Kathrein, H., Gonska, H. and Freund, F.: 1982, *Appl. Phys.* **30**, 33.

Kinoshita, K. and Yamada, T.: 1992, *Nature.* **357**, 313.

Mathez, E. A., Blacic, J. D., Berry, J., Maggiore, C. and Hollander, M.: 1987, *J. Geophys. Res.* **92**, 3500.

Mathez, E. A. and Delaney, J. R.: 1981, *Earth Planet. Sci. Lett.* **56**,

Mawhinney, T. P.: 1983, *J. Chrom.* **257**, 37.

Park, D. G., Martin, M. E., Ober, C. K., Burlitsch, J. M., Cavin, O. B., Porter, W. D. and Hubbard, C. R.: 1994, *J. Amer. Ceram. Soc.* **77**, 33.

Sadtler: 1987, in:*Sadtler Standard Spectra.* Baton Rouge, FL, Sadtler Research Laboratories.

Safonov, A. N., Lightowlers, E. C., Davies, G., Keary, P., Jones, R. and Öberg, S.: 1996, *Phys. Rev. Lett.* **77**, 4812.

Schrader, B. and Meier, W.: 1974,*Raman and IR Atlas of Organic Compounds*, Weinheim, Germany, Verlag Chemie.

Shaw, T. M., Dimos, D., Batson, P. E., Schrott, A. G., Clarke, D. R. and Duncombe, P. R.: 1990, *J. Mat. Res.* **5**, 1176.

Shimura, F., Hockett, R. S., Reed, D. A. and Wayne, D. H.: 1985, *Appl. Phys. Lett.* **47**, 794.

Silverstien, R. M., Bassler, G. C. and Morril, T. C.: 1974,*Spectroscopic Identification of Organic Compounds*, New York, NY, John Wiley & Sons, Inc.

Thompson, A. B.: 1992, *Nature.* **358**, 295.

Tingle, T. N., Mathez, E. A. and Hochella, M. F.: 1991, *Geochim. Cosmochim. Acta.* **55**, 1345.

Tsong, I. S. T., Knipping, U., Loxton, C. M., Magee, C. W. and Arnold, G. W.: 1985, *Phys. Chem. Minerals.* **12**, 261.
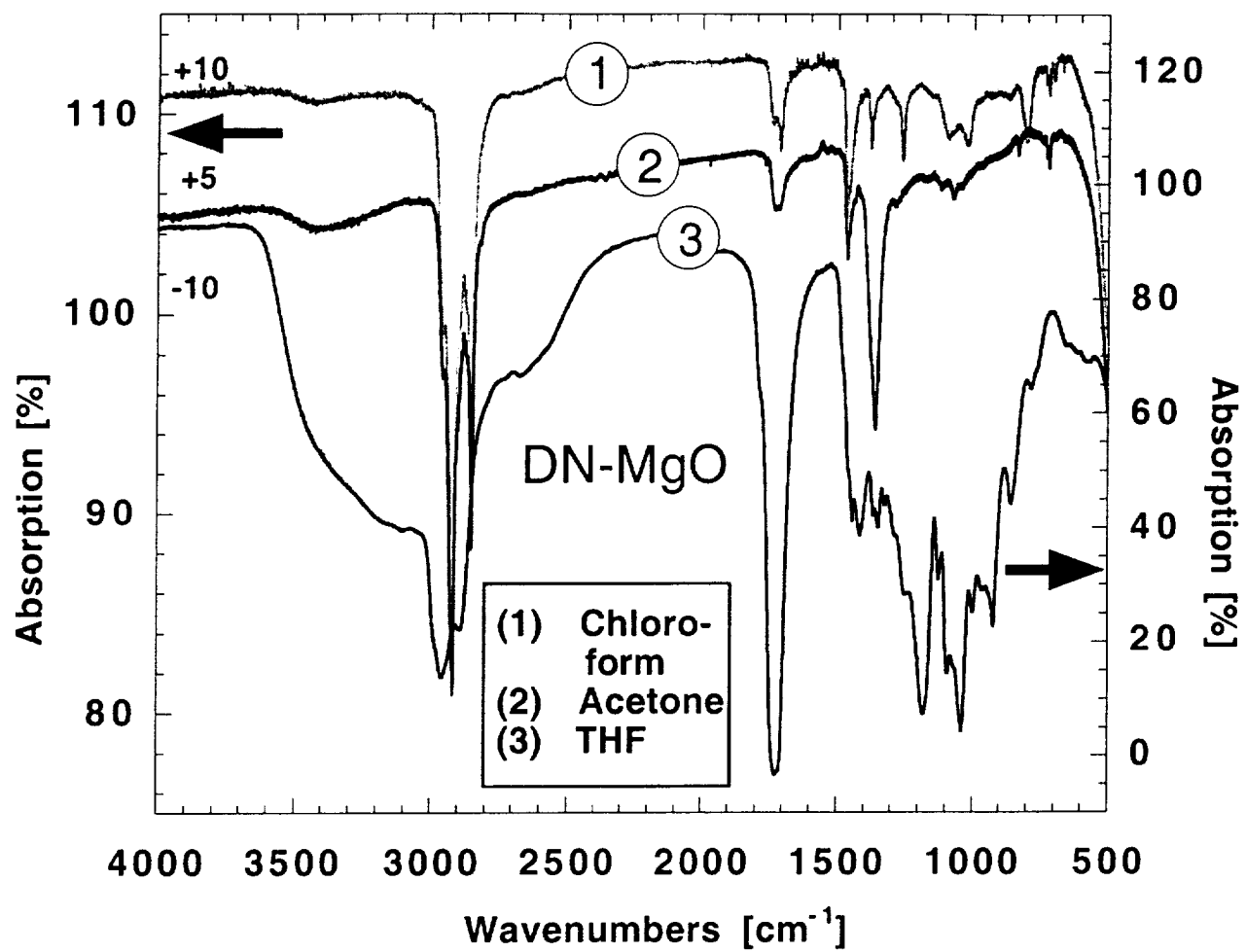
Warren, J. A., Smith, G. R. and Guillory, W. A.: 1980, *J. Chem. Phys.* **72**, 4901.

Weast, R. C. and Astle, M. J.: 1985, *CRC Handbook of Organic Compounds*, Boca Rouge, FL, CRC Press.

Wengeler, H., Knobel, R., Kathrein, H., Freund, F., Demortier, G. and Wolff, G.: 1982, *J. Phys. Chem. Solids.* **43**, 59.

Wilkins, R. W. T. and Sabine, W.: 1973, *Amer. Mineral.* **58**, 508.

(a)

(Figure 1a)

(b)
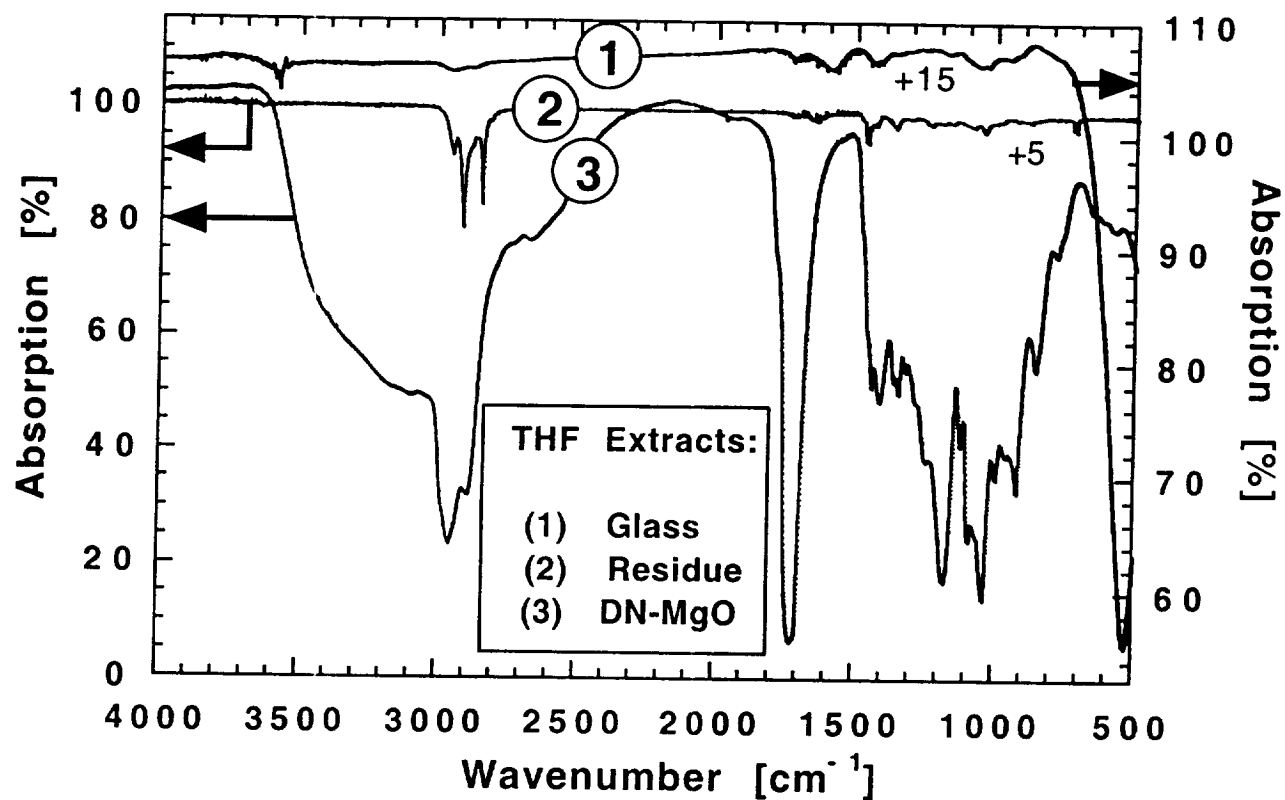
Figure 1: Infrared (IR) spectra **(a)** of the chloroform, acetone and tetrahydrofuran (THF) extracts of crushed MgO crystals grown by the arc fusion technique from a melt saturated with CO/CO_2, H_2O and N_2, and **(b)** of the THF extract of (1) crushed Pyrex glass (right scale), (2) THF residue (left scale), and (3) crushed MgO crystals (left scale). For clarity some IR spectra are vertically off-set by the amount indicated in %.
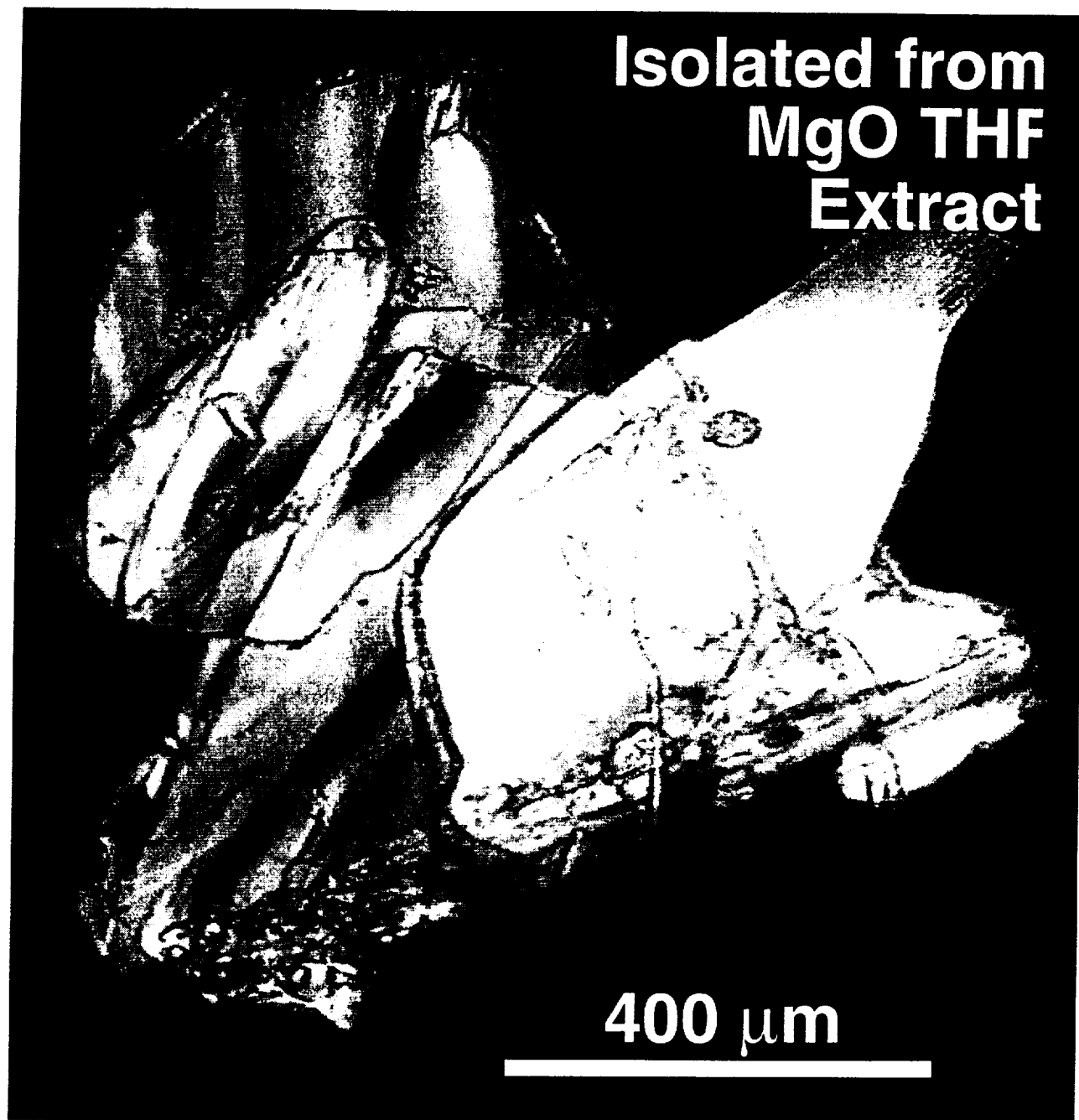
Figure 2: Succinic acid crystals grown from the purified THF MgO extract from chloroform solution.

IR Band Positions and Relative Intensities [Schrader and Meier 1974]

Wavenumber	Intensity
1690	very strong
1417	strong
1310	strong
1200	strong
1175	medium
917	strong
802	medium
634	strong
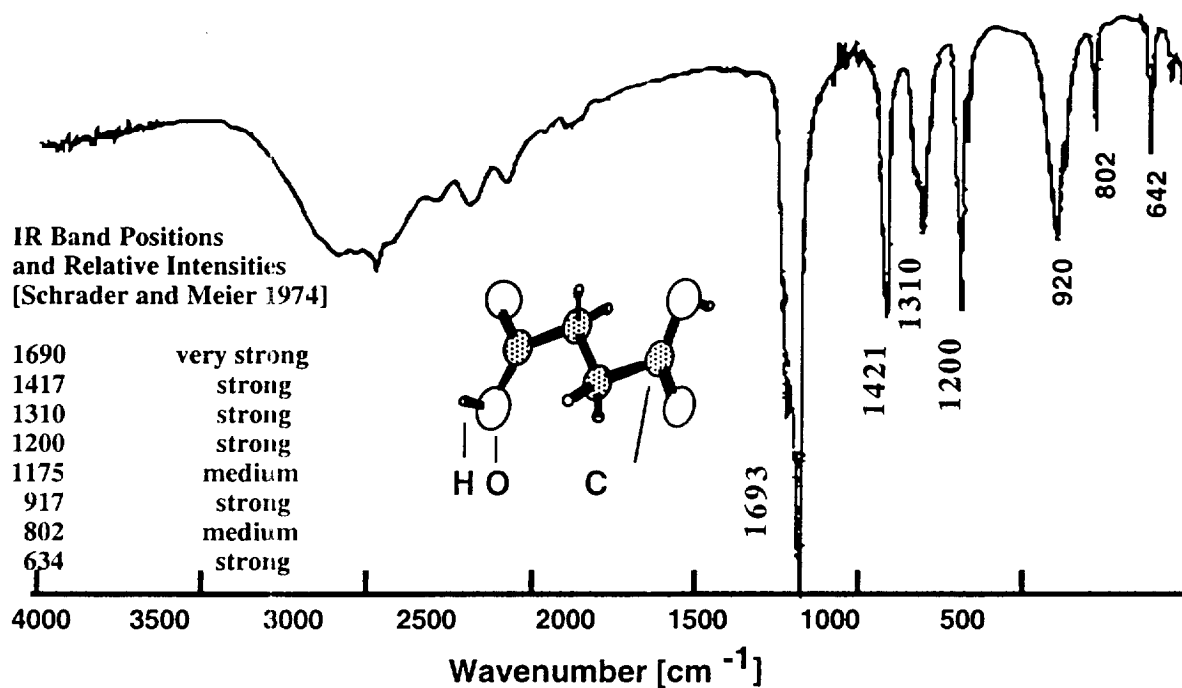
Figure 3: IR spectrum of the THF extract, purified through redissolution in chloroform. The positions and relative intensities of the measured IR bands are consistent with the published IR data for succinic acid, $HOOC(CH_2)_2COOH$ (inset table).
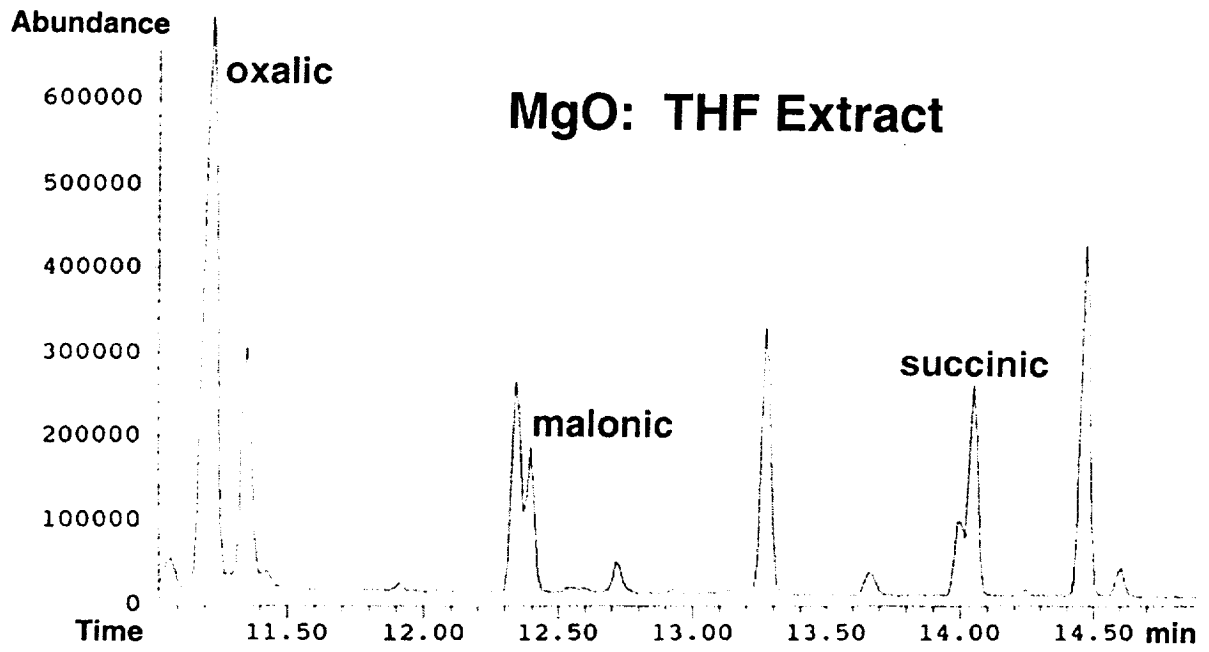
Figure 4: Gas Chromatogram trace (retention times 10 min to 15 min) of THF extract from MgO with three peaks assigned to dicarboxylic acids.
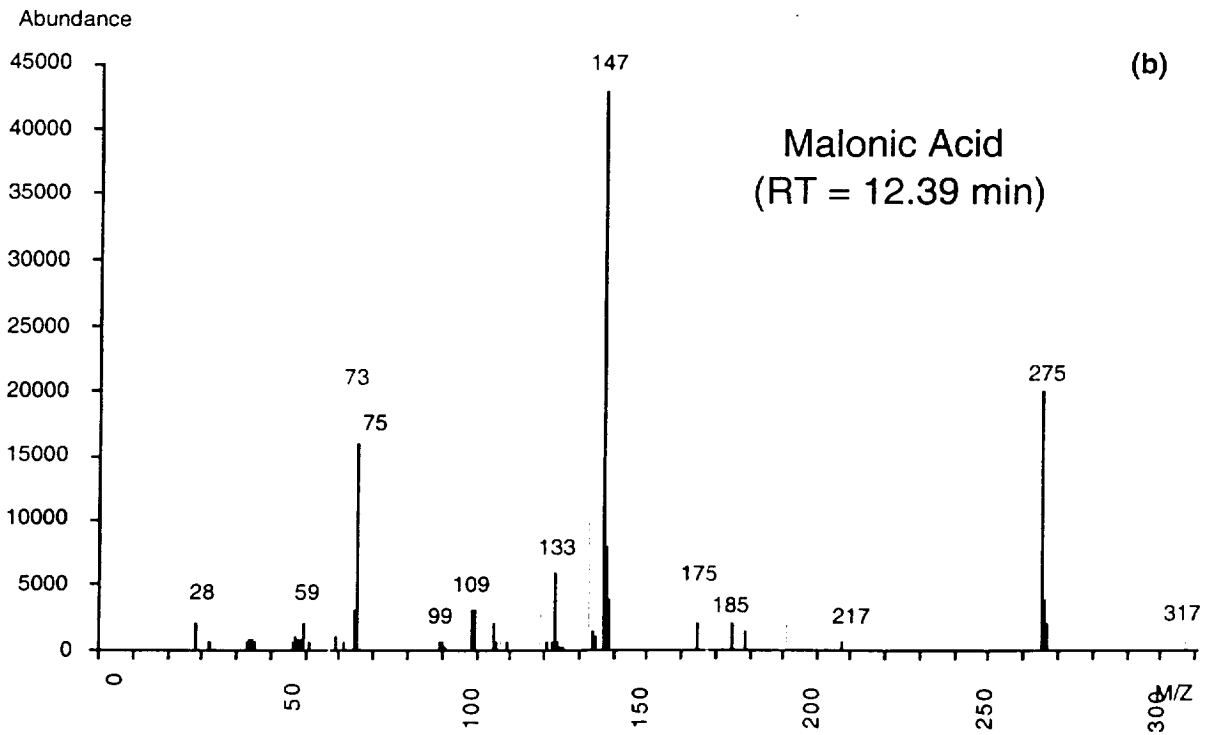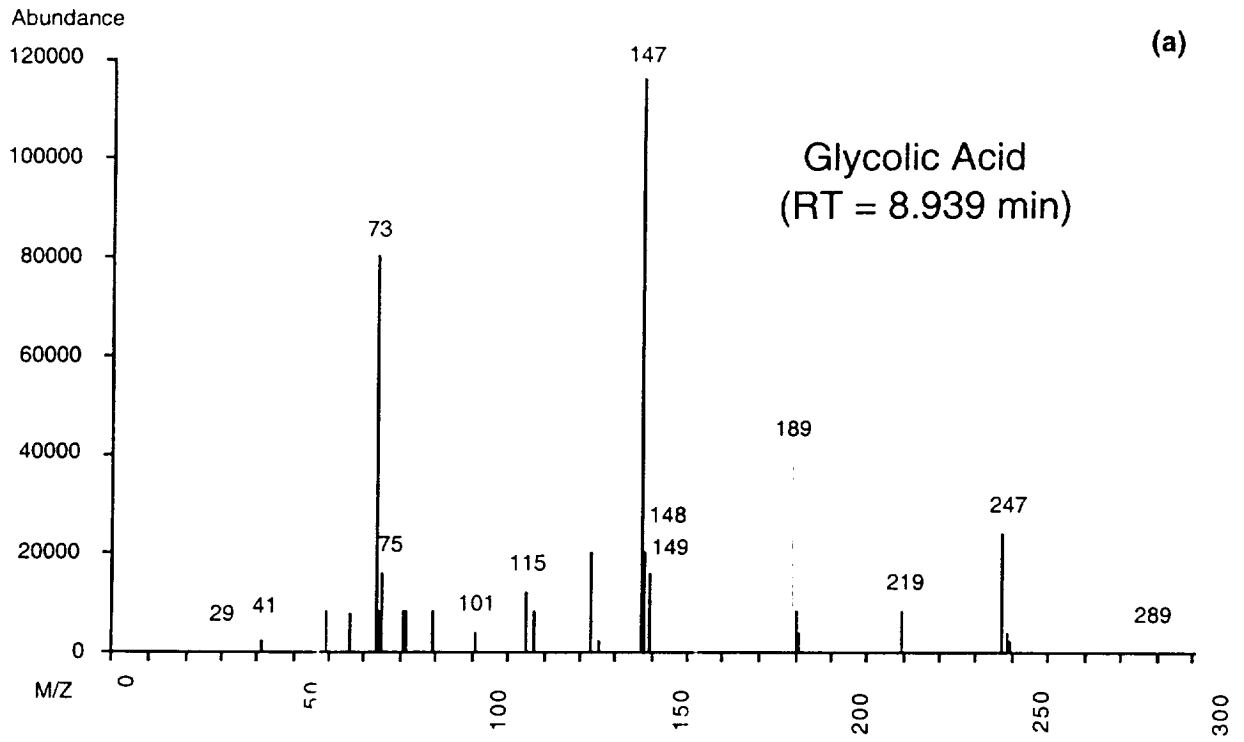
Figure 5a/b
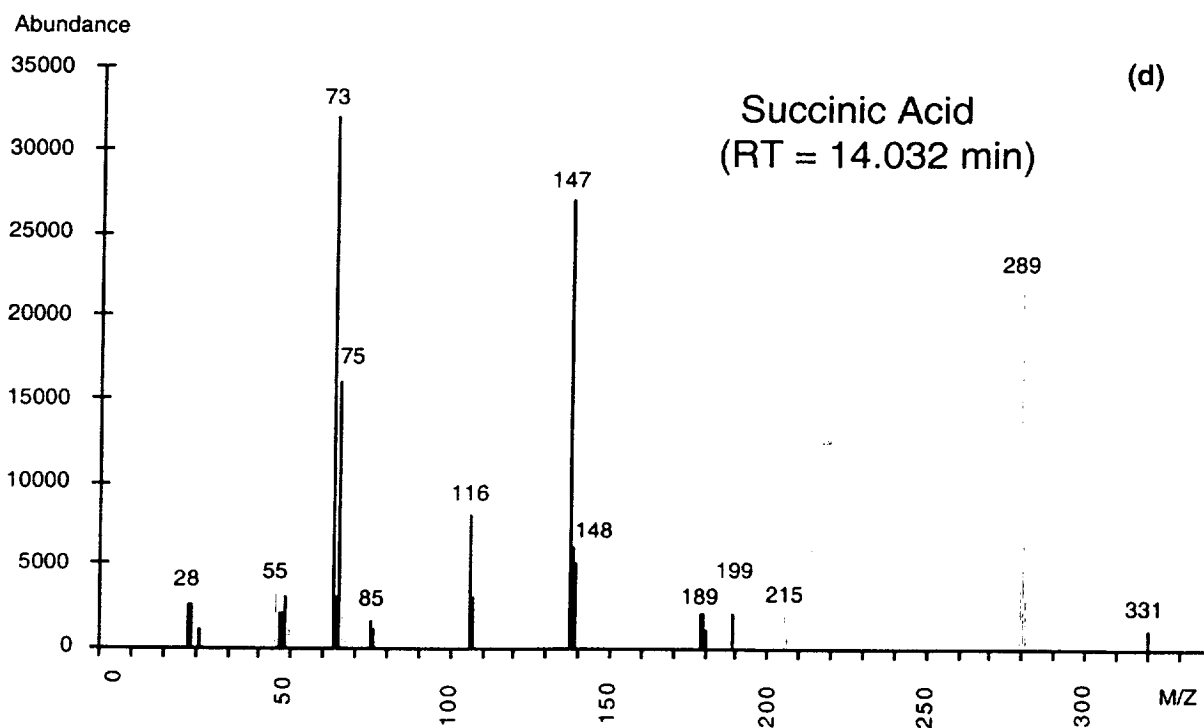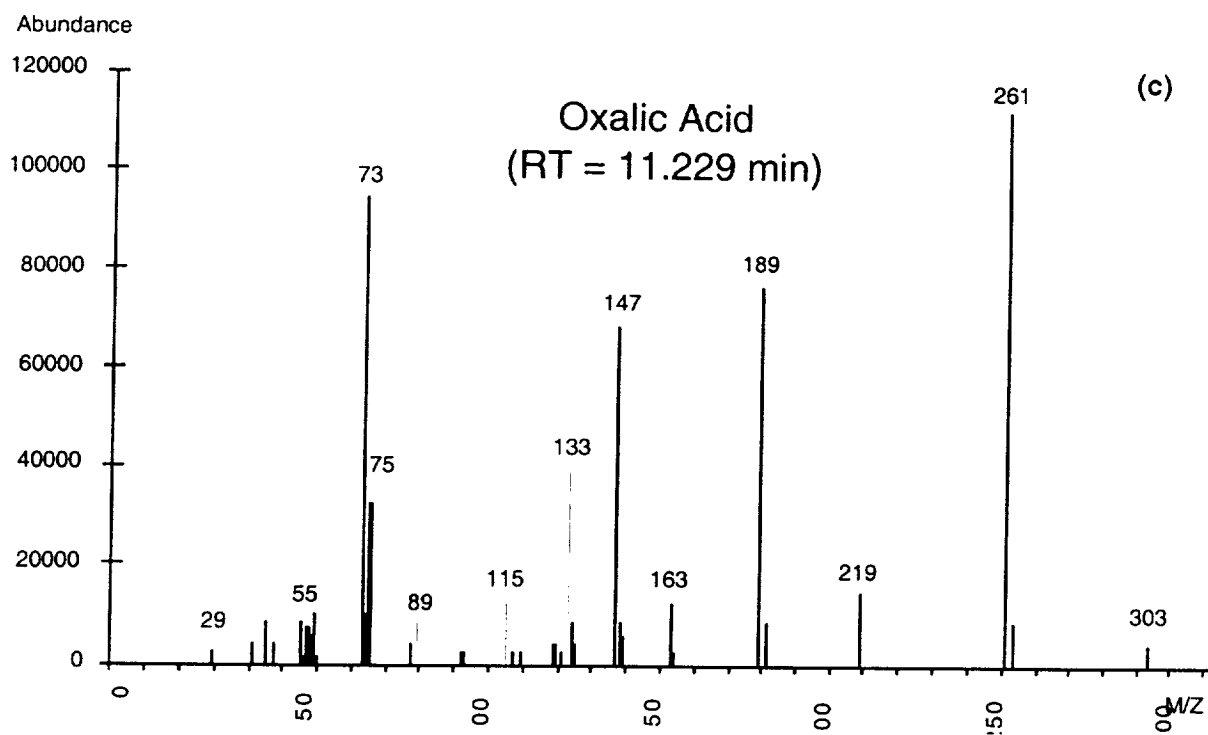
Figure 5a-d: Mass spectra of the four carboxylic and dicarboxylic acids identified in the THF extract from crushed MgO crystals.
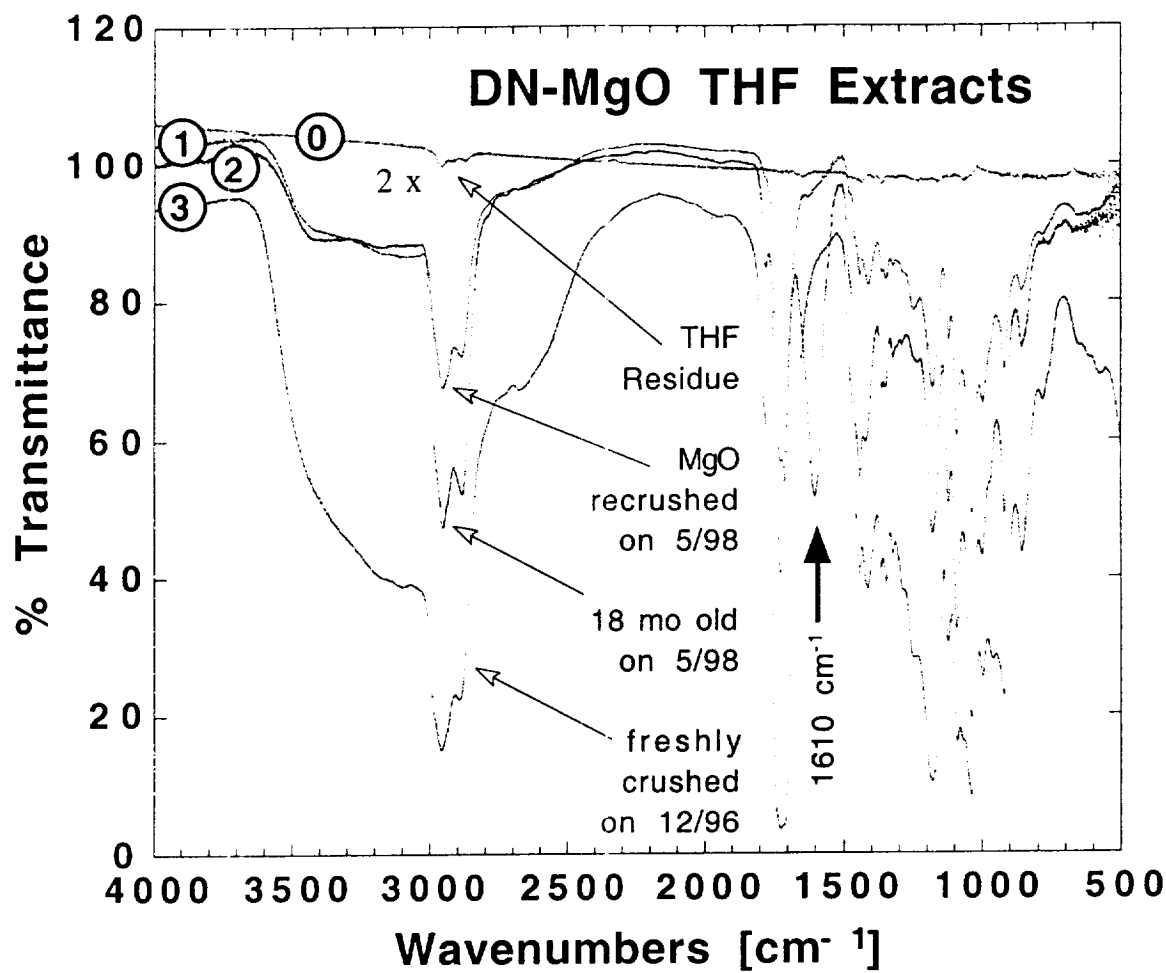
Figure 6: IR spectra of the THF solvent residue (0), magnified by a factor of 2, and of the THF extracts from MgO crystals: (1) freshly crushed, (2) after 18 months exposure to the laboratory atmosphere, and (3) after recrushing the 18 month old sample to a finer powder. All spectra were recorded from the dried residues of the THF extracts using the same amounts of MgO crystals for extraction, the same amount of THF solvent, and the same number of drops of the concentrated residues on the KBr disks.
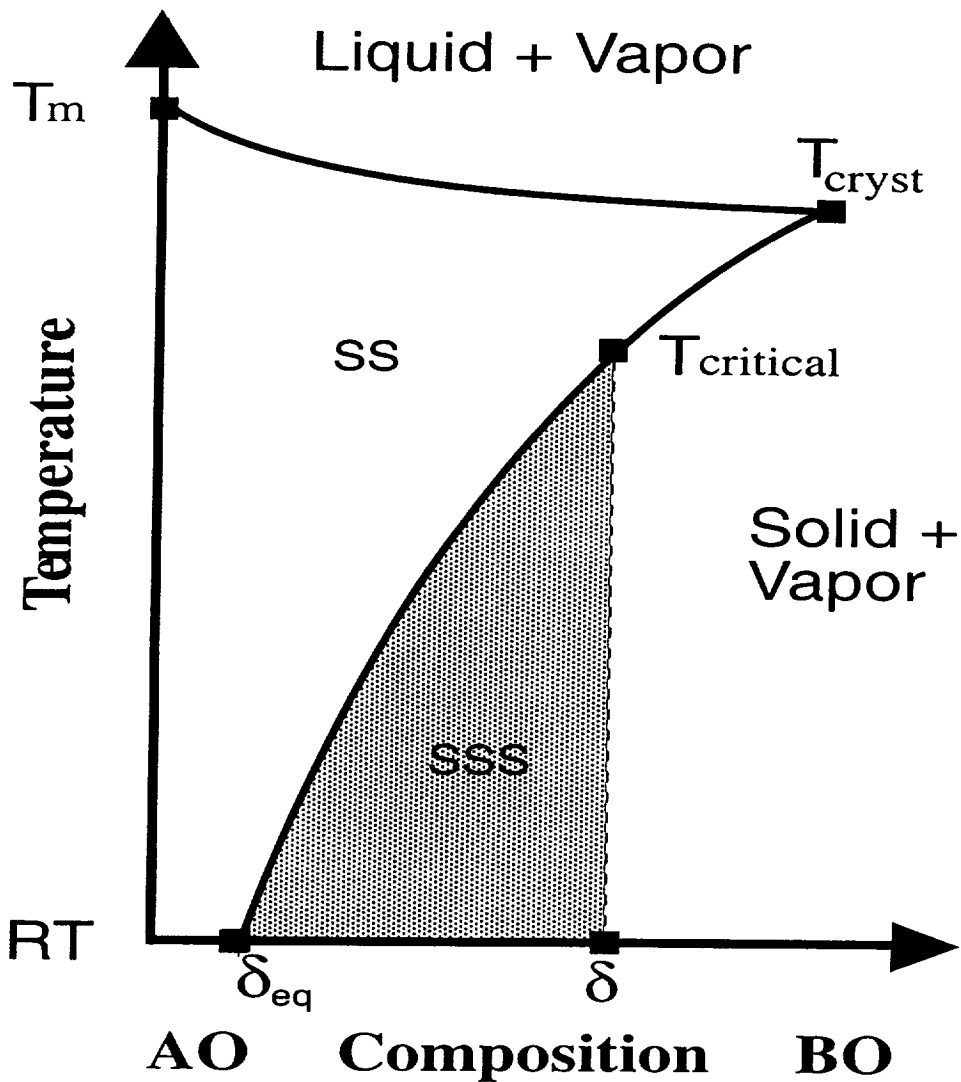
Figure 7: Partial phase diagram representative of a mineral AO crystallizing from a melt saturated with a gas or fluid phase BO. T_m: melting temperature of the "dry" AO; T_{cryst}: crystallization temperature of the AO-BO solid solution (ss). δ: amount of solute BO in the AO matrix of which δ_{eq} is the amount allowed under equilibrium conditions at room temperature (RT). $T_{critical}$: critical temperature at which the solid solution (ss) becomes supersaturated (sss).

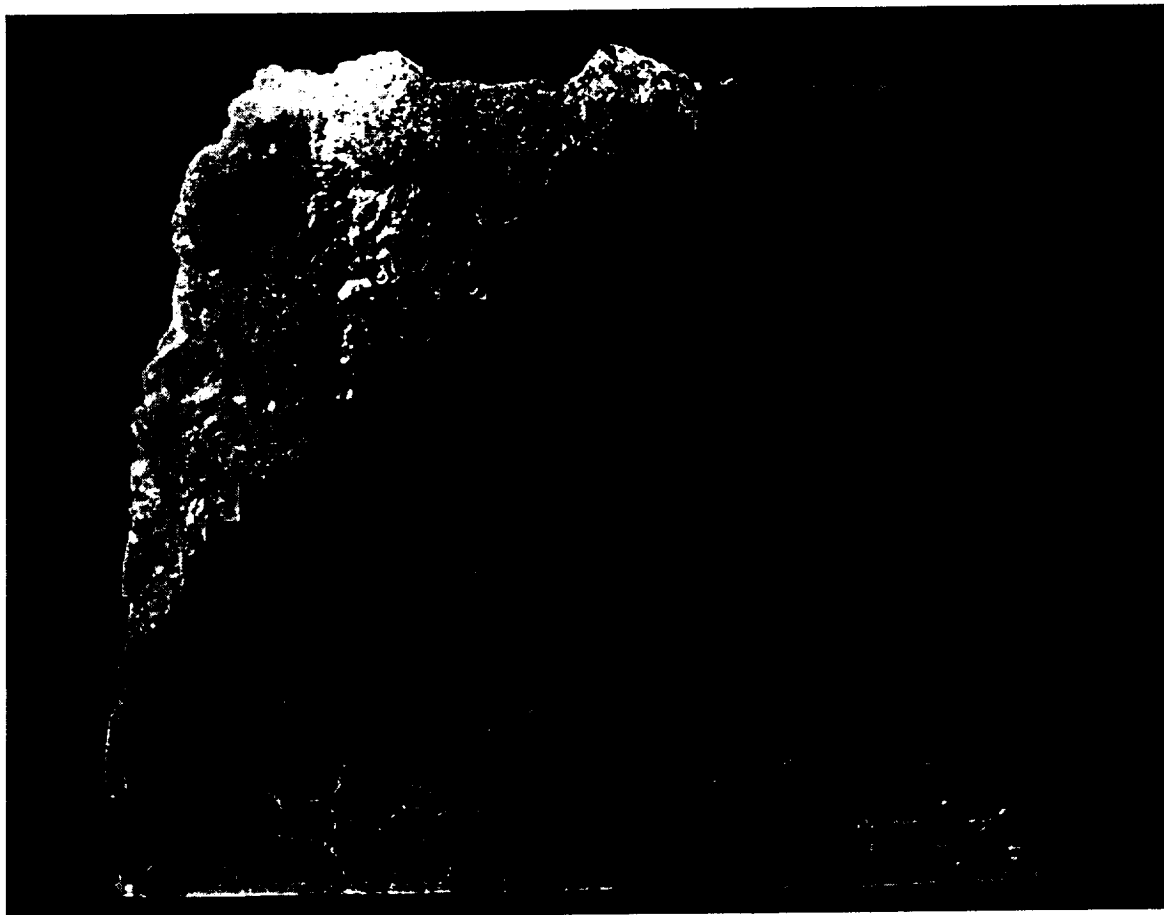# Melt–Grown 3N-MgO Single Crystal   —— 2 mm

Figure 8a: Large, high purity grade (99.9%) MgO single crystal, 20 mm at its base, 4 mm thick, with a clear rim and turbid interior. Top left: Chunk of the polycrystalline sintered MgO that had formed the wall of the MgO melt pool; Right: Part of the growth surface; Top and bottom: Cleaved faces.
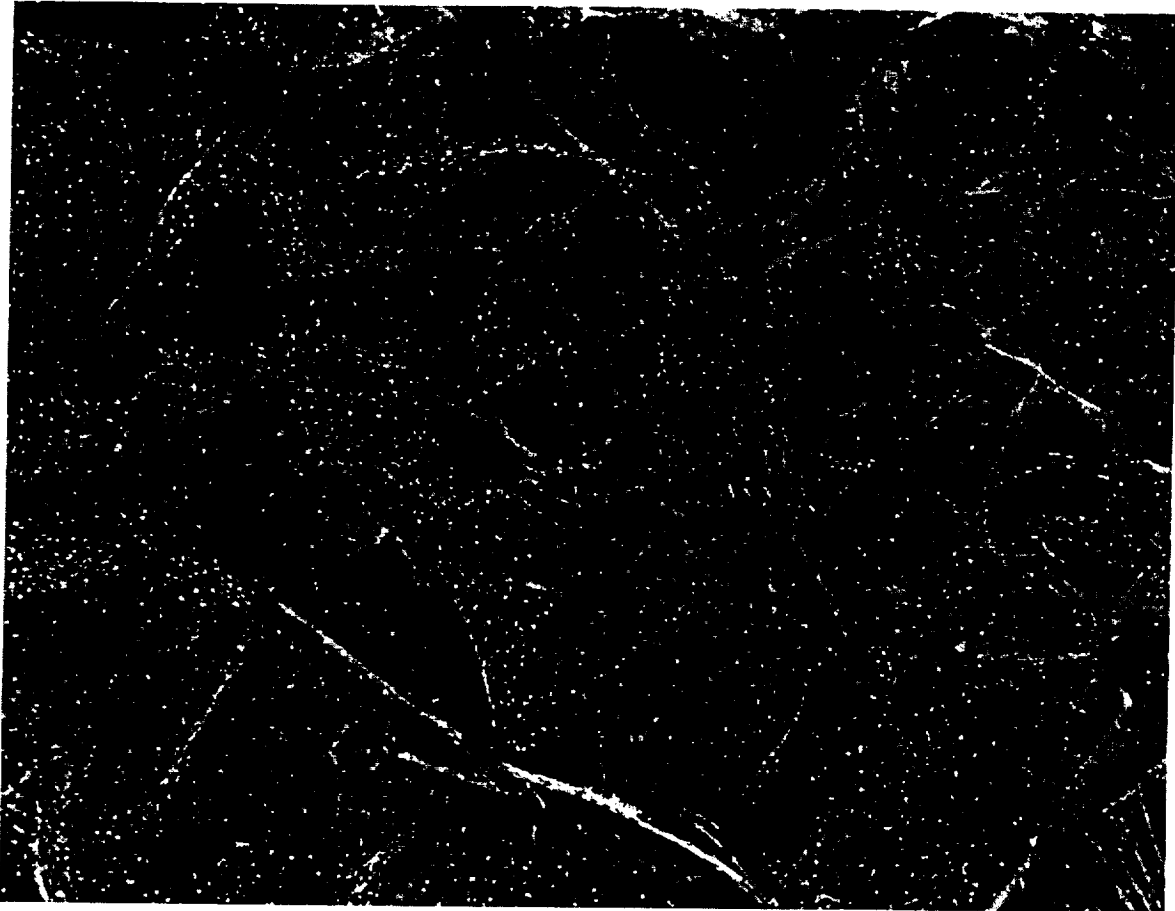
3N-MgO Cloudy Interior Region   —— 25 μm

Figure 8b: Interior region at higher magnification showing many isolated large cavities (5-10 μm) and subgrain boundaries decorated by millions of tiny cavities, presumably formed by vacancy clustering.
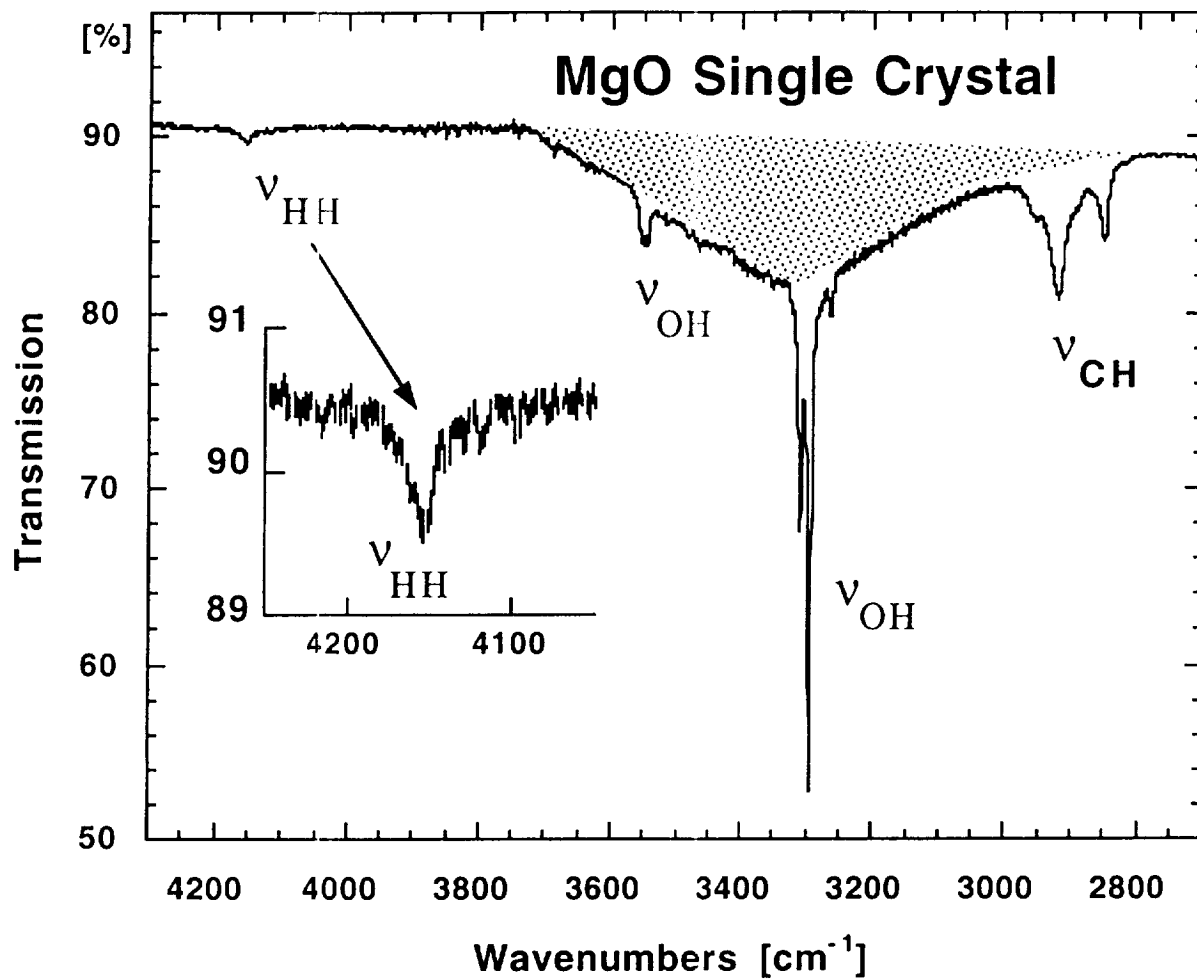
Figure 9: IR spectrum of an 8 mm thick turbid MgO single crystal, 99.9 % purity grade in the region of H–H, O–H, and C–H stretching frequencies.